# *P*-type macroporous silicon for two-dimensional photonic crystals

P. Bettotti,[a] L. Dal Negro, Z. Gaburro, and L. Pavesi
*INFM and Dipartimento di Fisica, Università di Trento, Via Sommarive 14, 38050 Povo-Trento, Italy*

A. Lui
*Istituto Trentino di Cultura–Istituto per la Ricerca Scientifica e Tecnologica, Via Sommarive 18, 38050 Povo-Trento, Italy*

M. Galli, M. Patrini, and F. Marabelli
*INFM and Dipartimento di Fisica "A. Volta," Università di Pavia, Via Bassi 6, 27100 Pavia, Italy*

(Received 10 May 2002; accepted 24 August 2002)

Macroporous silicon with two-dimensional periodicity has been produced by electrochemical etching, using a *p*-type doped silicon substrate. The structure shows photonic energy gaps in the infrared region, as demonstrated by variable angle reflectance measurements. The agreement between measurement and band calculations confirms the high quality of the samples. The use of an optimized electrolyte allows the fabrication of very high quality samples, with high aspect ratio and low roughness both at the surface and on the pore walls. The best results are obtained with aprotic and protophilic solvents. © *2002 American Institute of Physics.* [DOI: 10.1063/1.1515127]

## I. INTRODUCTION

Photonic crystals have attracted much interest in recent years.[1–3] The term photonic crystal indicates a structured material whose dielectric constant exhibits translation symmetry. Theoretical and experimental investigations show that such symmetry introduces energy bands in the photon dispersion which are reminiscent of the electronic band structure in electronic crystals. Suitable bases and lattices can also lead to forbidden energy gaps in photonic crystals. Photons with energy within such gaps cannot propagate through the material, thus suggesting possibilities for novel light-guiding structures and devices. A combination of photonic and electronic devices might be the optimal solution for a number of applications.[4,5] Therefore, techniques that allow fabrication of photonic crystals in Si hold the prospect of integration of photonic devices within complementary metal–oxide–semiconductor (CMOS) technology.

One way to fabricate two-dimensional photonic crystals in Si is by electrochemical anodization. The resulting material is commonly referred to as macroporous Si.[6] Spatial two-dimensional (2D) periodicity of pores can be obtained by defining a pattern of etch pits on the surface before anodization, for example, by photolithography. In this way, periodic arrays of equal cylindrical pores can be fabricated in a single pass, with constant diameter and very large aspect ratios, i.e., with pore depths hundreds of times larger than the pore diameters.

Large aspect ratios are possible because anodization is intrinsically an anisotropic process. In fact, according to a widely accepted etching model,[7] anodic dissolution of Si requires the presence of positive carriers (holes) at the Si–electrolyte interface. Also, during anodization, a space charge region (SCR) is set at the Si–electrolyte interface. The holes must cross the SCR to keep the etching going. Since the SCR is thinner and the electric field is larger in the pore tip regions, etching at the pore tip is faster than along the pore wall.[8]

The anisotropy of the anodization can be strongly enhanced in *n*-type substrates, because holes are minority carriers, and their concentration can be modulated over a wide range by external means. If no such external means are exploited, the hole population is negligible everywhere in the Si crystal, and the etching proceeds at a low rate. However, the etch rate increases if extra hole population is generated far from the pore region and diffuses towards the pores (e.g., by illuminating the backside of the wafer). By limiting hole generation, it is possible to collect the hole current completely at the pore tip. The etching at the pore wall is almost fully quenched in this case, and the aspect ratio can reach the amount of hundreds as above mentioned.[9] On the other hand, in *p*-type Si, the hole density cannot be controlled in the pore wall regions, and the macropores can only achieve the aspect ratio allowed by intrinsic anisotropy.[9]

It is interesting to investigate the anodization of *p*-type macroporous Si in order to obtain larger pore aspect ratios. Using *p*-type in place of *n*-type substrates has a number of advantages. First, the setup does not need illumination of the backside of the wafer to generate holes. Second, macroporous Si could further serve as the substrate for nanoporous silicon, whose formation also requires hole injection. An active medium could be then introduced into the pores by impregnating a nanoporous sponge.[10] Third, *p*-type substrates are largely preferred for CMOS processes, thus they are a natural choice for easier integration of photonic devices (e.g., waveguides, filters, etc.) with conventional electronics.

In this article we report experimental results that show how it is possible to grow very high aspect ratio photonic structures on *p*-type macroporous silicon using aprotic protophilic solvents, and how the dissolution mechanism of this substrate allows one to engineer the final aspect of the

[a]Electronic mail: bettotti@apha.science.unitn.it

 

macroporous lattice. The formation of photonic crystals is demonstrated by optical reflectance measurements.

## II. EXPERIMENT

We studied the formation of macroporous Si on *p*-type 100-oriented substrates with three different doping levels (0.1–0.2, 2–4, and 7–15 Ω cm) in order to demonstrate the existence of photonic gaps in the infrared (IR) spectral region. The electrolyte was optimized as described in earlier reports[11] using ethanol or two different organic aprotic protophilic solvents: dimethylformamide (DMF) and dimethylsulfoxide (DMSO). All solutions were prepared starting from HF 48 vol % in water and analytical grade reagents. Generally the composition of the electrolyte used is HF 4 M, diluted in ethanol, DMSO, or DMF. Etching was performed in an electrochemical cell, made of Teflon, with an area exposed to the electrolyte of $0.2\,\mathrm{cm}^2$.[12]

Both random and periodical macroporous Si were studied. For random samples, the Si surface was directly etched after cleaning in ethanol. For periodic structures, an etching mask was defined on the silicon surface using photolithography. Subsequent wet etching in KOH produced etch pits with a square shape. The final cross section of macropores becomes circular, indicating that in the plane perpendicular to pore axis anodization proceeds isotropically.

The samples were characterized by scanning electron microscopy (SEM) analysis using a JEOL 6100. The SEM images of random structures were analyzed by a two-step procedure. First, a transparent raster image was superimposed on the SEM image. This bitmap image was elaborated to produce a black and white image. In this way, we minimized errors due to application of a single threshold filter. Due to the limited gray-tone scale, a single threshold filter cannot distinguish between pores that do or do not develop in depth. The image was then processed by ScionImage Software Ver. 4.1b to obtain pore size distributions.

Optical characterization of the ordered macroporous samples was performed by variable angle reflectance (VAR) from the sample surface. VAR yields the photonic band dispersion.[13–15]. After polishing the sample surface to remove the etch pits, the VAR was measured in the spectral range of 0.2–1 eV by a Fourier-transform spectrometer (Bruker IFS66) at a spectral resolution of 1 meV and angular resolution of $\pm 1°$. The plane of incidence was chosen to be perpendicular to the sample surface and the angle of incidence $\theta$ was varied in the range of 5.4°–59.4° in steps of 5.4°. A liquid-nitrogen-cooled photoconductive HgCdTe was used as the detector and a silver mirror was used as the absolute reflectance reference. The photonic crystals had triangular lattice symmetry. Measurements were done for light incident along the $\Gamma$–*K* orientation of the 2D crystal, both in transverse electric (TE) and transverse magnetic (TM) polarizations by a polypropylene wire grid polarizer. In order to test the quality of the macroporous samples, the measured dispersion of the photonic bands was also compared with photonic bands calculated by means of standard plane wave expansion.[16,17]

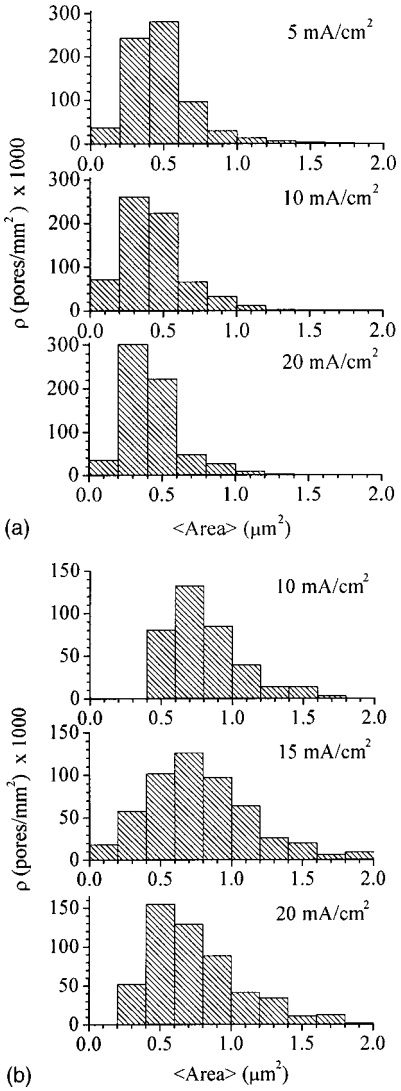


FIG. 1. Mean area vs current density. 2–4 Ω cm *p*-Si, HF 4 M, etching time 900 s. Top: DMF; bottom: DMSO.

## III. RANDOM MACROPOROUS SILICON

On Si wafers, anodic dissolution yields random pore distribution where the pore dimension varies randomly and the pore size depends on the doping density. To compare different electrolytes and to determine the average properties of the resulting structures, their morphological properties versus etching conditions were studied.

As an example, Fig. 1 shows histograms of pore areas in random macroporous samples obtained on 2–4 Ω cm *p*-type doped Si wafers. Remarkably, the mean area and its distribution were dependent on the specific organic electrolyte used but not on the etching current density.

The silicon etching rate was strongly dependent on the solvent used (Fig. 2). The main difference in etching rate concerns the comparison between ethanoic and DMSO solutions. From the data of Fig. 2(a), we could estimate etch rates of 0.1 and of 0.7 $\mu$m/min for ethanoic and DMSO electrolytes, respectively, associated with a $10\,\mathrm{mA/cm}^2$ current density. This is a significant difference. A comparison between the organic solvents [Fig. 2(b)] showed a small difference in

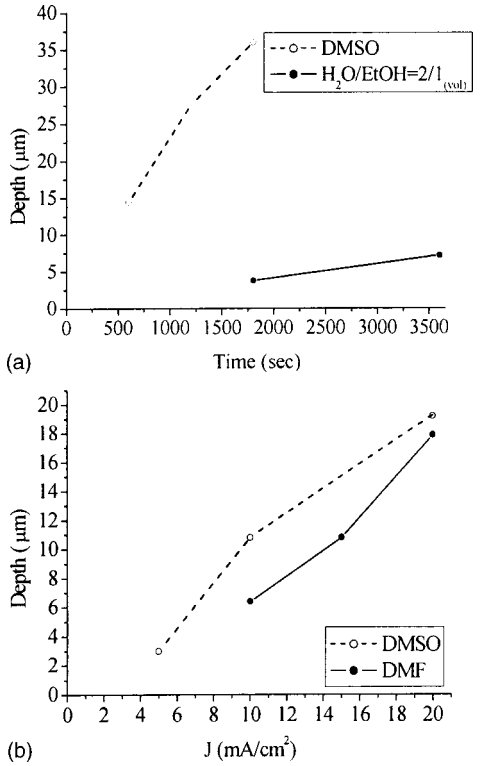


FIG. 2. Etch rate dependence on solvent, etching time, and current density. In (a) the current density was kept constant at 10 mA/cm$^2$. In (b) the etching time was kept constant at 900 s. Both are on *p*-Si 7–15 Ω cm. The error bars on the depths determined are 0.1 $\mu$m.

etch rate, always less than 50%, and evidence of a reduction in the etch rate for DMSO when the current was increased.

Another difference between the DMF and the DMSO electrolytes was the range of density of current span. Using DMF and current density lower than 10 mA/cm$^2$ it was not possible to obtain macroporous structures that retain pores topology in depth, instead of what was obtained with DMSO. In addition, with DMSO the mean area was about 0.45 $\mu$m$^2$ (pore radius of 0.38 $\mu$m) and the filling factor was between 27% and 37%, whereas with DMF the mean area was about 0.8 $\mu$m$^2$ (pore radius of 0.5 $\mu$m) and the filling factor was between 35% and 42%.

The role of the solvents in the silicon etching mechanism is not yet clear.[7] There are at least two facts to consider: (i) DMSO and DMF solvate differently the ions in the solution in a way more effective than water and ethanol;[18,19] (ii) the polarization of the semiconductor–electrolyte interface is modified by the presence of aprotic solvents.[7] This could influence the extent of the SCR inside the semiconductor since the extension of the double layer inside the electrolyte is changed. A rough estimate of the interface polarization could be made by simply looking at the voltage across the cell during the anodic etch. Even though the measurements were not referred to a third electrode, we believe that the values are significant because of the great difference in the area of the working (0.2 cm$^2$) and counter (20 cm$^2$) electrodes and the low polarizability of the platinum counterelectrode.[20,21] In water the junction bias was about 0.8 V; with DMF it increased to about 1.4 V, and in DMSO the junction bias was 20 V. DMSO acts as a better solvent for HF with respect to DMF in macroporous silicon formation both because it produces pores in a larger range of current densities and because it forms smaller pores in random samples. Thus, DMSO is promising for obtaining photonic crystals with a gap at 1.5 $\mu$m.

## IV. ORDERED MACROPOROUS SILICON

Pre-patterned substrates anodized using the ethanoic electrolyte always exhibited significant pore wall etching. On the contrary, the use of aprotic solvents showed very interesting effects. It was possible to reduce the resistivity of the substrate from more than 10 to 0.1 Ω cm where high aspect ratio periodic structures can be formed. In addition, using the same lithographic mask, different structures could be obtained using different etching conditions. The influence of the change of electrolyte was studied using a square lattice of etch pits with lattice constants from 10 to 1 $\mu$m and with a ratio pore diameter/lattice constant equal to 2. When patterned 7–15 Ω cm substrates were etched with the ethanoic solvent, the etch pits developed into macropores. Interestingly, for a lattice constant of 10 $\mu$m, pores in an interstitial position have also been obtained [Fig. 3(a)]. No predefinition of etch pits was required for such interstitial pores. The pore in the interstitial position appeared whenever the thickness of the wall between two adjacent pores was larger than twice the depletion width of the electrolyte/silicon junction. At this stage no reliable measurements of the depth of the interstitial pores have been made. Evidence of lateral etching is also evident when a tilted view of the macroporous sample is observed [Fig. 3(b)].

The sample surface became undulated. In addition, the square lattice of the pores turned into a square lattice of pillars when the lateral growth of pores was such that nearby pore walls were consumed. Figures 3(c)–3(e) show progressive dissolution of the pore walls for decreasing lattice constants from 4 to 2 $\mu$m. The structures obtained using the ethanoic electrolyte do not have high aspect ratio because of widening of the pores.

This picture changed when aprotic solvents like DMF or DMSO were used due to the more anisotropic character of the attack, as shown in Fig. 4. No evolution from the pore to the column lattice was observed, at least not at the scale of these dimensions. This indicates diminished importance of the lateral etching. On the square lattice with large lattice parameters, like the one shown in Fig. 4(a), a random distribution of small macropores formed in the interstitial regions of the ordered lattice of large macropores. The macropore dimension is determined by the etch pits in the ordered region and by the substrate resistivity in the region where random macropores occur. This effect has been named the proximity effect and was studied in Ref. 22.

Interstitial pores form in lattices with shorter period (6 $\mu$m) when using aprotic solvents compared to the minimum period required with ethanoic solution (10 $\mu$m). This is further evidence of the reduction of the space charge region for DMSO or DMF.

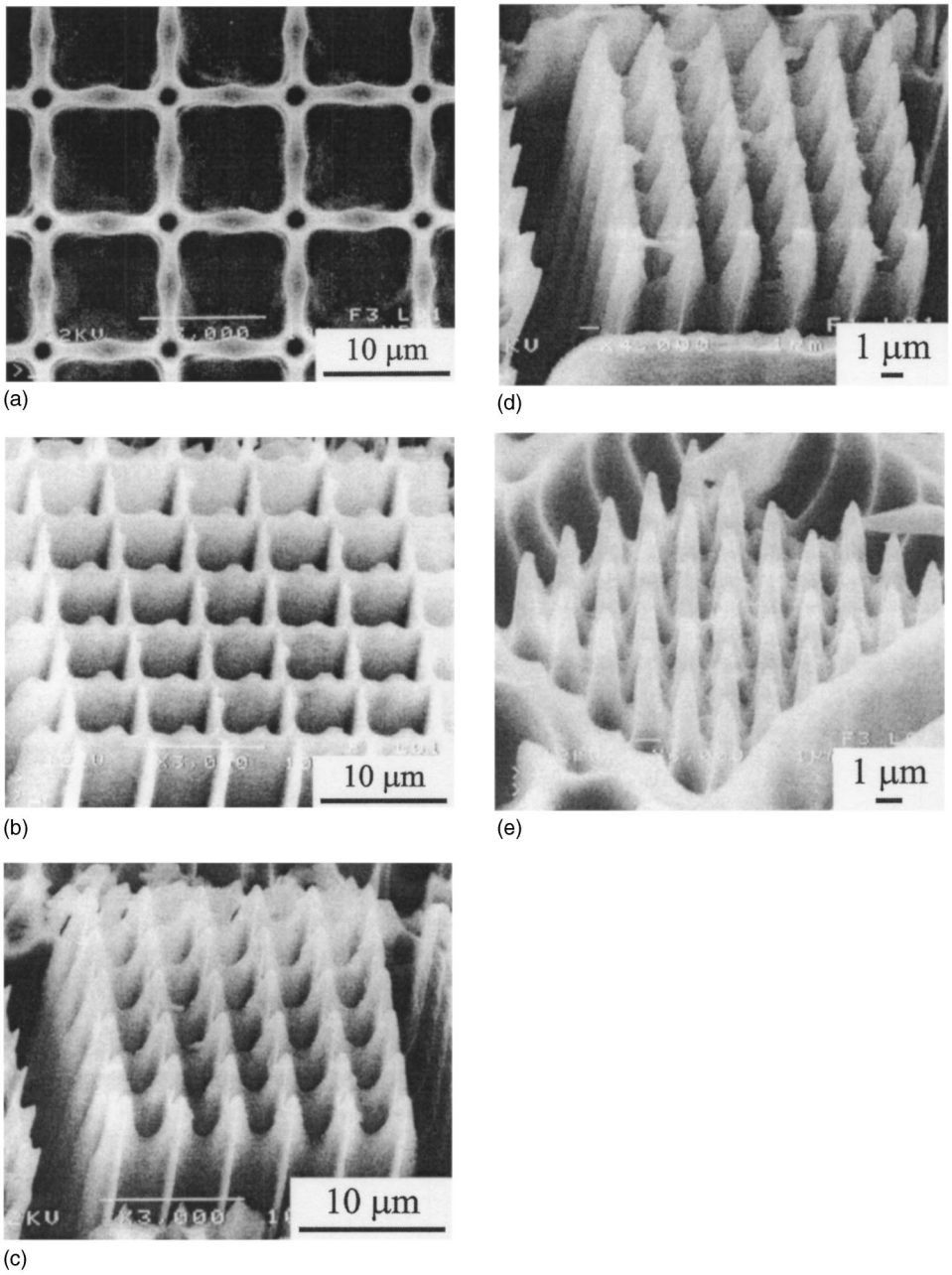


FIG. 3. SEM images of ordered macropore samples obtained on *p*-type doped Si with 7–15 Ω cm resistivity with HF 3 M ethanoic solution. The etching current was 10 mA/cm$^2$ for 2400 s. The lattice constants are (a) 10, (b) 6, (c) 4, (d) 3, and (e) 2 $\mu$m.

By reducing the lattice parameter, better control of the square macropore lattice was obtained [Figs. 4(c)–4(e)]. It is interesting to note that the lattice with the smallest lattice constant of 1.5 $\mu$m [Fig. 4(e)] never developed with ethanoic solutions. The ethanoic solutions tended to dissolve the lattice completely, also because of the long etching time needed to produce small pores.

The proximity effect occurred for smaller lattice constants in more conductive substrates when aprotic solution was used. Again, this could be considered a result of the different SCR: in the sample shown in Fig. 5(a) the thickness of the pore walls is greater than the sum of the two SCR and interstitial pores, whereas for the same lattice parameter and etching conditions no interstitial pore forms in a more resistive substrate like the one in Fig. 4(c). In 2–4 Ω cm substrates, no macropores formed when ethanoic solutions were used. On the contrary, with the organic solvent all the starting patterns we defined could be transferred (Fig. 5).

Another important difference between samples etched in ethanoic solutions with respect to those etched with aprotic solutions is the planarity of the surface. When ethanoic solutions were used, an enhancement of the etch rate at the corners of the square lattice was observed, which caused an undulated texture of the sample surface. This effect was not noticed with aprotic solvents. In this case a flat sample surface was obtained which suggests effective passivation of the silicon surface exposed to the solution.

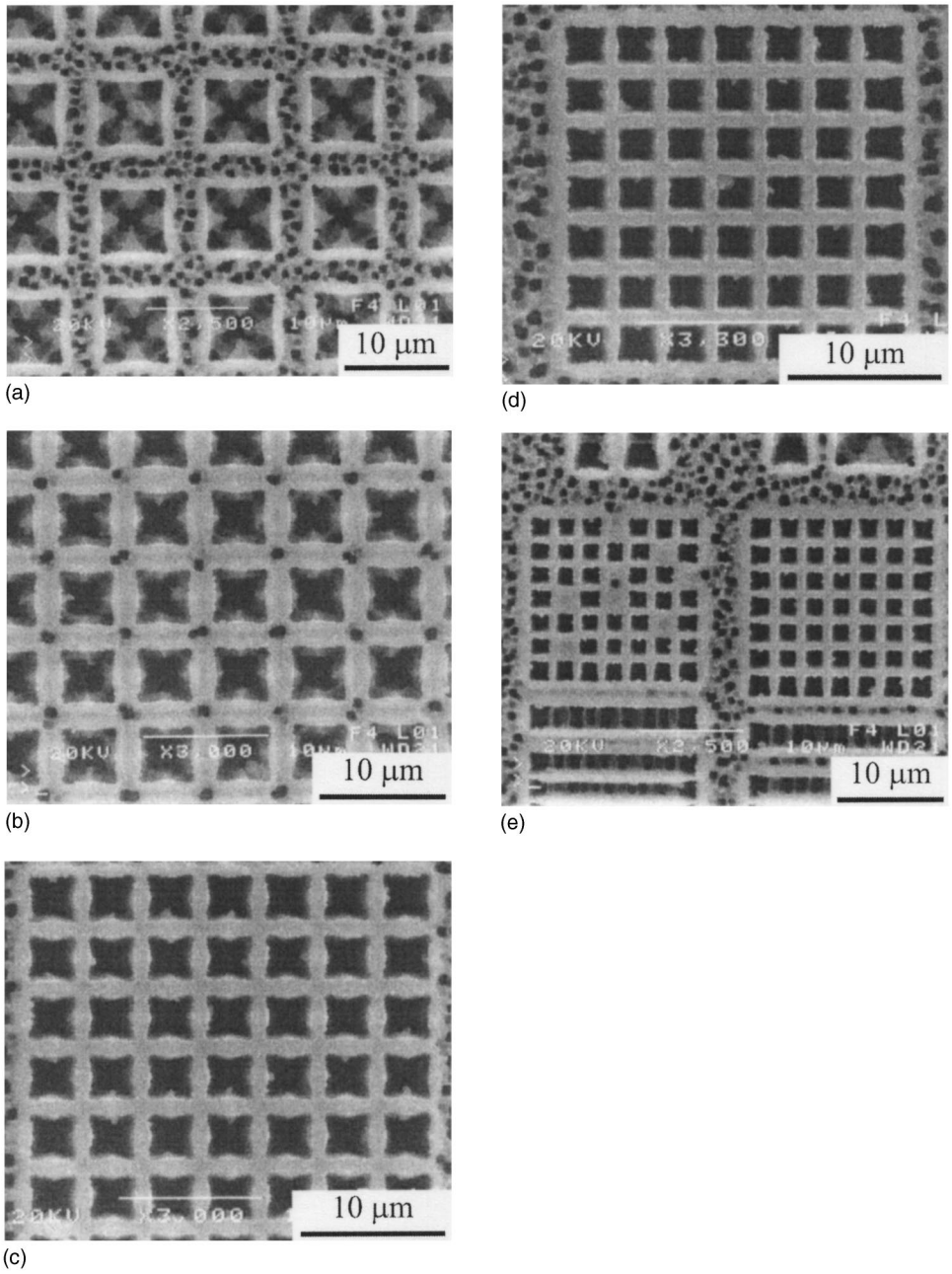


FIG. 4. SEM images of ordered macropore samples obtained on *p*-type doped Si with 7–15 Ω cm resistivity with HF 4 M DMSO solution. The etching current was 10 mA/cm$^2$ for 900 s. The lattice constants are (a) 10, (b) 6, (c) 4, (d) 3, and (e) 2 (right) and 1.8 $\mu$m (left). The lack of some macropore in (e) was due to little development of the mask in the lithographic process.

## V. PHOTONIC CRYSTALS ON *p*-TYPE SILICON

The superior performance of the aprotic electrolyte can be used to obtain photonic crystals with *p*-type doped Si. A triangular lattice of etch pits was written on high resistivity substrates (7–15 Ω cm) with different lattice parameters. By electrochemical etch, the lattice was transferred into Si. Figure 6 shows two examples. The structures are very regular with a maximum aspect ratio of about 40. This aspect ratio is not the limiting value for these etching conditions. In the literature values as large as 100 have been reported.[23] A comparison is possible with macroporous silicon obtained on *n*-type doped substrates.[24] The main difference we noticed concerns the final shape of the etch pits defined by the wet KOH etching. On *p*-type doped samples the walls are almost vertical even near the surface, whereas on the *n*-type doped substrate inverted pyramidal shaped pores are observed after the etch, which are remnants of the initial pits. This is due to the more anisotropic etch for *n*-type than for *p*-type substrates, even when aprotic electrolytes are used for *p*-type substrates.

To test the photonic properties of the structures obtained, variable angle reflectance measurements from the sample surface were performed. Figure 7 shows the results for a sample etched in DMF. Results are given for TE- and TM-polarized light incident along the $\Gamma$–$K$ orientation. As previously reported and discussed for *n*-type macroporous Si

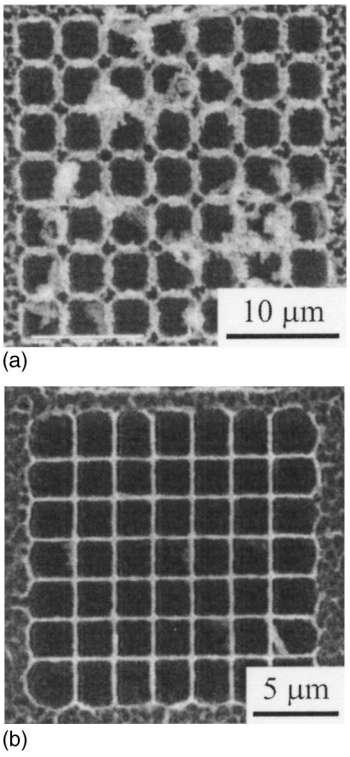


FIG. 5. SEM images of ordered macropore samples obtained on *p*-type doped Si with 2–4 Ω cm resistivity with HF 4 M DMSO solution. The etching current was 10 mA/cm$^2$ for 900 s. The lattice constants are (a) 4 and (b) 1.8 $\mu$m.

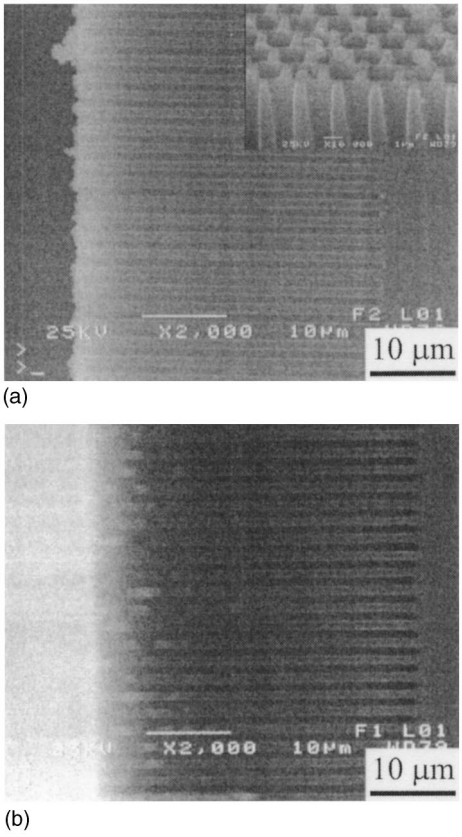


FIG. 6. SEM images of ordered macropore samples obtained on *p*-type doped Si with 7–15 Ω cm resistivity with HF 4 M (a) DMSO (b) DMF solution. The etching current was 10 mA/cm$^2$ for 1800 s. The lattice constant is 2 $\mu$m.

based photonic crystals,[24] the angular dependent reflectance is characterized by prominent step-like features that display well-defined dispersion as a function of the incidence angle $\theta$. These are associated with the excitation of photonic modes in the photonic crystal and may be regarded as ''absorption'' processes that give rise to spectral line shapes similar to those of one-dimensional (1D) critical points in semiconductors. Each structure in reflectance marks the onset of a diffracted beam which propagates in the material whenever the frequency $\omega$ of the incident wave and the parallel wave vector $k_{\parallel}=(\omega/c)\sin\theta$ match those of an allowed photonic mode in the photonic crystal. Notice in particular the strong feature at 0.3 eV at the lowest angle of incidence $\theta=5.4°$ for both TE and TM polarizations: this corresponds to a mode that has the same symmetry of the light field at the $\Gamma$ point.[17,24]

From experimental reflectance spectra, the dispersion of the photonic bands in a given direction can be extracted by plotting the energy positions of the observed step-like features versus the parallel wave vector $k_{\parallel}$. Two-dimensional photonic bands are commonly separated in *E* modes (field components $E_z, H_x, H_y$) and *H* modes (field components $H_z, E_x, E_y$) according to mirror symmetry with respect to the *xy* plane, i.e., the plane perpendicular to the holes.[17] However, since either TE-polarized or TM-polarized incident light can interact with both *E* and *H* modes,[24] a better comparison with calculated bands is obtained when the photonic bands are classified according to mirror symmetry with respect to the vertical plane of incidence, i.e., the plane of polarization of the incident lightwave. Photonic bands extracted from TE-polarized reflectance are therefore compared to bands which are odd with respect to this mirror plane, while those extracted from TM-polarized reflectance are compared to bands, which are even.

The analysis is shown in Fig. 8, where the measured dispersion of photonic bands for TE polarization (odd modes) and TM polarization (even modes) is shown together with the calculated one for the $\Gamma$–K direction. For the calculations the parameters of the photonic crystal extracted from

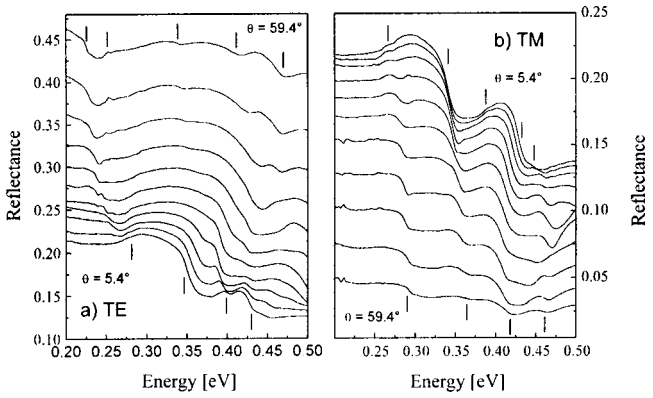


FIG. 7. Experimental reflectance of sample DMF17 (lattice constant $a=2$ $\mu$m, air fraction $r/a=0.3$) for light incident along the $\Gamma$–K orientation for (a) TE polarization and (b) TM polarization. Vertical bars mark the positions of 2D photonic modes for 5.4° and 59.4°.

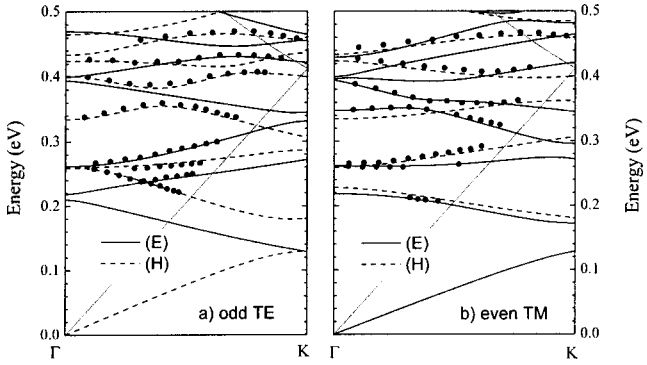


FIG. 8. Solid points: Measured dispersion of the photonic bands derived from structures in reflectance spectra; solid and dashed lines: photonic bands separated according to parity with respect to the plane of incidence. (a) TE polarization, odd modes; (b) TM polarization, *H* modes. The dispersion of free photons is indicated by dotted lines.

SEM analysis were used. The remarkable agreement between the experimental points and calculated bands of proper parity as well as the observation of peculiar features typical of the photonic band structure, i.e., anticrossing between bands of the same symmetry, clearly demonstrate the high quality of these *p*-type macroporous silicon photonic crystals.

## VI. CONCLUSIONS

The main difference between etching of *p*- and *n*-type silicon by HF stems from lateral growth of the pores. Lateral growth is almost absent in *n*-type Si while it is present in *p*-type Si. This means that the final macroporous structures on *p*-type Si are influenced by the current density, the HF concentration, and the duration of the etching process. Lateral growth is large when ethanoic solutions are used. Indeed, pillar lattices can be obtained by a square lattice of etch pits. On the contrary, the addition of a suitable organic electrolyte to HF allows one to produce good photonic crystals, with aspect ratio comparable to that obtained in the *n*-type substrate. Although a detailed explanation of this effect is still under debate, here we pointed out the role of the decreased space charge region. We tested two aprotic solvents, DMF and DMSO. Both solvents give high quality macropore samples. However, DMF is more hazardous than DMSO and the etch rate is smaller for DMF than for DMSO. Hence DMSO appears to be a better choice. Variable angle reflectance shows the good quality of the photonic crystals produced and is confirmed to be a suitable technique with which to characterize 2D photonic crystals.

## ACKNOWLEDGMENT

This work was partially supported by MURST through PRIN 2000 project "One- and Two-Dimensional Photonic Crystals: Growth, Theory, and Optical Properties."

[1] S. Fan, A. Mekis, S. G. Johnson, and J. D. Joannopoulos, AIP Conf. Proc. **560**, 57 (2001).
[2] S. Boscolo, M. Midrio, and C. G. Someda, IEEE J. Quantum Electron. **38**, 47 (2002).
[3] L. Po-Tsung, J. R. Cao, C. Sang-Jun, W. Zhi-Jian, J. D. O'Brien, and P. D. Dapkus, IEEE Photonics Technol. Lett. **14**, 435 (2002).
[4] K. Kato and Y. Tohmori, IEEE J. Sel. Top. Quantum Electron. **6**, 4 (2000).
[5] A. V. Krishnamoorthy and K. W. Goossen, IEEE J. Sel. Top. Quantum Electron. **4**, 899 (1998).
[6] J. Schilling *et al.*, J. Opt. A, Pure Appl. Opt. **3**, S121 (2001).
[7] The dissolution process of Si in fluoride media is not fully understood. Different mechanisms were proposed since the 1980s. A very complete source of information is X. G. Zhang, *Electrochemistry of Silicon and its Oxide* (Kluwer Academic, Dordrecht, The Netherlands, 2001).
[8] V. Lehmann and H. Föll, J. Electrochem. Soc. **137**, 653 (1990).
[9] V. Lehmann and S. Rönnebeck, J. Electrochem. Soc. **146**, 2968 (1999).
[10] P. Bettotti, M. Cazzanelli, L. Dal Negro, B. Danese, C. J. Oton, G. Vijaya Prakash, and L. Pavesi, J. Phys. C **14**, 1 (2002).
[11] S. Lust and C. Levy-Clement, Phys. Status Solidi A **182**, 17 (2000).
[12] O. Bisi, S. Ossicini, and L. Pavesi, Surf. Sci. **38**, 1 (2000).
[13] V. N. Astratov, D. M. Whittaker, I. S. Culshaw, R. M. Stevenson, M. S. Skolnick, T. F. Krauss, and R. M. De La Rue, Phys. Rev. B **60**, R16255 (1999).
[14] V. N. Astratov, I. S. Culshaw, R. M. Stevenson, D. M. Whittaker, M. S. Skolnick, T. F. Krauss, and R. M. De La Rue, J. Lightwave Technol. **17**, 2050 (1999).
[15] V. N. Astratov, R. M. Stevenson, I. S. Culshaw, D. M. Whittaker, M. S. Skolnick, T. F. Krauss, and R. M. De La Rue, Appl. Phys. Lett. **77**, 178 (2000).
[16] J. D. Joannopoulos, R. D. Meade, and J. N. Winn, *Photonic Crystals* (Princeton University Press, Princeton, NJ, 1995).
[17] T. Ochiai and K. Sakoda, Phys. Rev. B **63**, 125107 (2001).
[18] M. Chalaris and J. Samios, J. Mol. Liq. **78**, 201 (1998).
[19] J. F. Tyler, D. Patey, and G. N. Patey, J. Chem. Phys. **110**, 10937 (1999).
[20] G. Ives and G. J. Janz, *Reference Electrodes, Theory and Practice* (Academic, New York, 1961), p. 71.
[21] P. Bettotti, Graduation thesis, University of Padua, Italy, 2000, p. 45.
[22] A. Vyatkin, V. Starkov, V. Tzeilin, H. Presting, J. Konle, and U. König, J. Electrochem. Soc. **149**, G70 (2002).
[23] K. J. Chao, S. C. Kao, C. M. Yang, M. S. Hseu, and T. G. Tsai, Electrochem. Solid-State Lett. **3**, 489 (2000).
[24] M. Galli *et al.*, Phys. Rev. B **65**, 113111 (2002).